

AE Aquarii: how CVs descend from supersoft binaries

K. Schenker¹, A.R. King¹, U. Kolb², G.A. Wynn¹, Z. Zhang^{1,2,3}

¹ *Theoretical Astrophysics Group, Department of Physics and Astronomy, University of Leicester, Leicester, LE1 7RH, U.K.*

² *Department of Physics and Astronomy, The Open University, Walton Hall, Milton Keynes, MK7 6AA, U.K.*

³ *National Astronomical Observatories, Chinese Academy of Sciences, Beijing 100012, P.R. China*

Accepted. Received

ABSTRACT

AE Aquarii is a propeller system. It has the shortest spin period among cataclysmic variables, and this is increasing on a 10^7 yr timescale. Its UV spectrum shows very strong carbon depletion vs nitrogen and its secondary mass indicates a star far from the zero-age main sequence. We show that these properties strongly suggest that AE Aqr has descended from a supersoft X-ray binary. We calculate the evolution of systems descending through this channel, and show that many of them end as AM CVn systems. The short spindown timescale of AE Aqr requires a high birthrate for such systems, implying that a substantial fraction of cataclysmic variables must have formed in this way. A simple estimate suggests that this fraction could be of order one-third of current CVs. We emphasize the importance of measurements of the C/N abundance ratio in CVs, particularly via the C IV 1550/N V 1238 ratio, in determining how large the observed fraction is.

Key words: novae, cataclysmic variables — binaries: close — stars: evolution — stars: individual: AE Aqr — abundances — stars: individual: AM CVn

1 INTRODUCTION

AE Aqr is one of the most distinctive cataclysmic variables (CVs). It has a long orbital period of 9.88 hr (Welsh et al., 1993), and the shortest coherent pulse period (33 s), increasing on a timescale $\sim 10^7$ yr (de Jager et al., 1994). Doppler tomography reveals the apparent absence of an accretion disc. This has led to its interpretation as a ‘propeller’ system (Wynn et al., 1997): the white dwarf is apparently expelling centrifugally the matter transferred from the companion. To arrive at such a highly non-equilibrium spin rate, the mass transfer rate in the recent (10^7 yr) past must have been much higher than its current value $\dot{M}_2 \sim \text{few} \times 10^{-9} M_\odot \text{yr}^{-1}$, and decreased on a still shorter timescale. IUE spectra of AE Aqr (Jameson et al., 1980) reveal the most extreme C IV to N V ratio of all CVs (Mauche et al., 1997), probably indicating strong carbon depletion and thus CNO cycling. The short spin period makes the system effectively a double-lined spectroscopic binary, with masses $M_1 \simeq 0.89 \pm 0.23 M_\odot$ for the white dwarf (WD) and $M_2 \simeq 0.57 \pm 0.15 M_\odot$ for the donor star (Welsh et al., 1995; Casares et al., 1996). The donor star is of spectral type K5V (Welsh, 1999) which is too late for the given orbital period and too early for the measured M_2 if it is on the main sequence.

We show here that all of these properties are consistent

with the idea that AE Aqr descends from a supersoft X-ray binary, cf. Schenker & King (2002). The thermal-timescale mass transfer characterizing such sources ends once the secondary/primary mass ratio $q = M_2/M_1$ decreases sufficiently, leading to a rapid transition to normal CV evolution driven by angular momentum losses, cf. King (1988). If the white dwarf is magnetic, as in AE Aqr, the high mass transfer rate in the thermal-timescale phase will have spun it up to a short spin period. This must lengthen rapidly in order to reach equilibrium with the lower transfer rate in the CV state, and this spindown is what drives its propeller action. The very short lifetime of the propeller phase implies a high birthrate for such systems, comparable to those of known CVs. This in turn suggests that systems descending from evolutions like AE Aqr must constitute a large fraction of all CVs.

The simple idea that all CVs form with essentially unevolved, low-mass main sequence (MS) donors has been repeatedly challenged for more than a decade (Pylyser & Savonije, 1988a,b; Baraffe & Kolb, 2000; Schenker, 2001; King & Schenker, 2002; Schenker & King, 2002). If mass transfer starts with mass ratio $q \gtrsim 1$ the secondary’s Roche lobe R_L tends to shrink with respect to its thermal-equilibrium radius R_{TE} . Mass is therefore transferred on a thermal timescale ($\sim \text{few} \times 10^7$ yr), at rates high enough

to sustain steady nuclear burning on the material accreted by the white dwarf, and thus explain (short-period) super-soft X-ray sources (van den Heuvel et al., 1992; King et al., 2001).

After this relatively brief phase, q becomes small enough that R_L shrinks more slowly than R_{TE} , and thermal-timescale mass transfer ends. The systems either evolve off to longer orbital periods, driven by nuclear evolution, or switch to stable, angular-momentum-loss-driven mass transfer like ordinary CVs. We will show that AE Aqr is at the end of this transition phase to a CV, accounting for its strange properties. AE Aqr is passing through this transition very rapidly; its whole evolution up to its current state is short compared to the stable CV phase afterwards. In this sense AE Aqr is not unique at all: a significant fraction of CVs must descend from similar evolutions.

In the next section we derive some rough estimates for the potential progenitor system of AE Aqr, using a simplified analytic description of the orbital evolution during rapid mass transfer. Sect. 3 studies the behaviour of single star models under fixed mass loss of the order expected during such an evolution. This allows us to identify the influence of varying stellar parameters, and establish whether the observed properties of AE Aqr are compatible with this scenario. We present a set of full binary evolution calculations in Sect. 4 and discuss them in Section 5. Section 6 is the Conclusion.

2 SIMPLIFIED ORBITAL EVOLUTION

To get a first idea about the required initial parameters for the progenitor system of AE Aqr, we recall that during thermal-timescale mass transfer additional angular momentum losses (magnetic braking & gravitational radiation) are negligible compared to the changes of the Roche radius resulting from mass transfer itself, e.g. King et al. (2001). We define η by

$$\dot{M}_1 = -\eta \dot{M}_2 \quad (1)$$

as the fraction of the mass lost from the secondary that is actually accreted on to the WD, while assuming that the rest leaves the system with average specific angular momentum equal to the primary's, i.e. $\beta = 1$ in the nomenclature of King et al. (2001). From their eq. (10) we obtain the evolutionary tracks as

$$\frac{P}{P_i} = \left(\frac{M_{2i}}{M_2}\right)^3 \left(\frac{M_i}{M}\right)^2 \left(\frac{M_{1i}}{M_1}\right)^{3/\eta} \quad (2)$$

and

$$\frac{R_2}{R_{2i}} = \left(\frac{M_{2i}}{M_2}\right)^{5/3} \left(\frac{M_i}{M}\right)^{4/3} \left(\frac{M_{1i}}{M_1}\right)^{2/\eta} \quad (3)$$

respectively for $\eta > 0$. For the limit $\eta = 0$ these lead to the exponential expressions given e.g. in King & Ritter (1999).

Equipped with these expressions we can estimate where analytically computed curves for the evolution of radius and orbital period intersect those describing mass loss under the assumption of permanent thermal equilibrium (i.e. essentially along the MS). These intersections mark the transition between the fast thermal-timescale mass transfer (super-soft) and CV-like angular-momentum-loss-driven evolution at lower mass transfer rates. Figure 1 shows a set

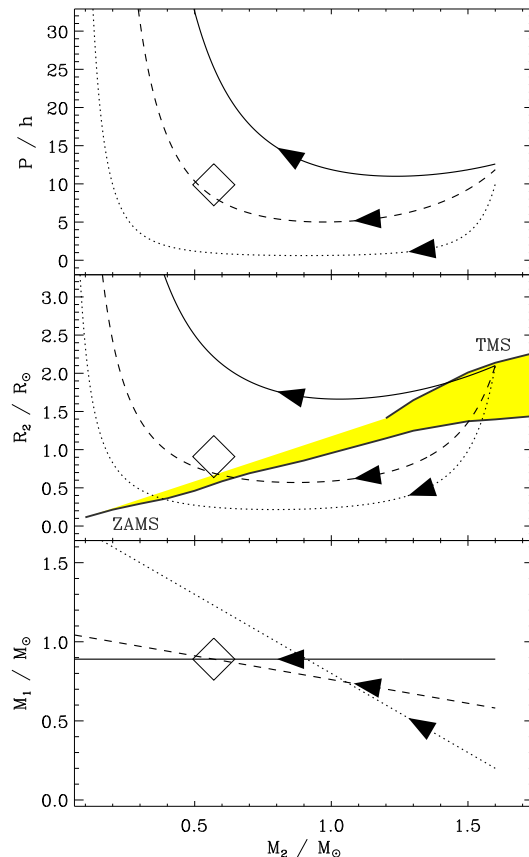


Figure 1. Evolution of a model AE Aqr progenitor system. For the assumed parameters and $M_{1,\text{now}} = 0.89 M_{\odot}$, various tracks are shown, starting from a $1.6 M_{\odot}$ star which has almost reached its maximal MS radius. The three panels show the evolution of the orbital period, secondary radius and WD mass for different cases (dotted line: $\eta = 1$ — full line: $\eta = 0$ — dashed line: $\eta = 0.3$). The diamond marks the current position of AE Aqr. Note that the conservative model ($\eta = 1$) cannot meet the requirements for M_1 : even starting from the lowest plausible WD mass, it has grown well beyond the Chandrasekhar limit before reaching the current P_{orb} of AE Aqr. The grey shaded area in the middle panel marks the radii of single stars during their main sequence life as labelled.

of curves for different η together with the shaded location of the MS framed by a pair of thick curves marking the zero-age MS (ZAMS) and the turn-off MS (TMS). For the latter we use the point of maximal radius prior to core hydrogen exhaustion. Note that this definition is not applicable to MS stars without convective cores (i.e. with masses below $\sim 1.2 M_{\odot}$). The lowest panel shows the growth of the WD mass as the donor evolves (from right to left) for various η . The initial WD mass M_{1i} is chosen so that the current position of AE Aqr is reached with masses of $(M_1, M_2) = (0.89 M_{\odot}, 0.57 M_{\odot})$ in accordance with observation. A good fit should also pass through the correct orbital period and radius (estimated by the corresponding period – mean density relation). The assumption of fully conserva-

tive mass transfer ($\eta = 1$) leads to much higher WD masses than observed, and we therefore do not consider it further.

Using the curves shown we derive first guesses for the system parameters of the progenitor system, i.e. M_{1i} , M_{2i} , and η . We cannot expect these estimates to be very precise, as the actual reaction of the system to mass loss in this transition phase follows neither the Roche curves nor the equilibrium curves (the secondary is out of thermal equilibrium).

Nevertheless we can estimate $M_{2i} \sim 2 M_{\odot}$ and $1.5 \lesssim q_i \lesssim 3$, where the upper constraint derives from the occurrence of delayed dynamical instabilities (DDI, see King et al. (2001) and discussion section). As explained above, conservative mass transfer gives too high a WD mass. However a value $\eta \simeq 0.3$ is plausible and gives an M_1 mildly increased over the average field WD mass, in accordance with observations of AE Aqr.

3 SINGLE STAR CALCULATIONS

We have shown that in principle a recent thermal–timescale mass transfer supersoft phase could explain AE Aqr. We now use full stellar models. This determines the star’s reaction to mass loss, and thus whether the observed spectral type (SpT) may be reached in this way. We simplify the mass transfer history as

$$-\dot{M}_2 = \begin{cases} M_2/\tau_{\text{KH}} & \forall M_2 > M_{\text{sw}} \\ 2 \times 10^{-9} M_{\odot}\text{yr}^{-1} & \forall M_2 \leq M_{\text{sw}} \end{cases} \quad (4)$$

where τ_{KH} is the secondary star’s Kelvin–Helmholtz time, thus mimicking thermal–timescale mass transfer and the subsequent transition to an evolution driven by angular momentum loss, as in ordinary CVs. The switching mass M_{sw} is chosen so that thermal–timescale mass transfer ends when $q \simeq 1$, i.e. it can be roughly identified with M_1 . A more thorough discussion of the exact stability conditions in CVs is presented in Webbink (1985); Sobermann et al. (1997).

The code we use in both the single star case of the last Section and the binary calculations reported here is based on Mazzitelli (1989), as adapted by Kolb & Ritter (1992) plus minor improvements. The mapping from effective temperature to SpT follows the procedure outlined in Beuermann et al. (1998) and Baraffe & Kolb (2000). This is not entirely self-consistent as our code still uses grey atmospheres.

At first we performed a number of calculations for Pop. I stars with 1.2, 1.6 and $2.0 M_{\odot}$ and initial ages of 0, 0.25, 0.5, 0.75 and 1 of their MS-lifetime, using a switching mass of $M_{\text{sw}} = 1 M_{\odot}$. As shown in Fig. 2, more massive stars of the same evolutionary phase and further evolved stars of the same mass will both lead to larger equilibrium radii after the thermal–timescale mass transfer.

Single star radii can easily be converted into orbital periods by equating to the corresponding Roche radius (with a primary mass given by M_1). This allows us to compare our tracks with the observed parameters for AE Aqr, $P_{\text{orb}} = 9.88$ hr, SpT = K5 and $M_2 = 0.57 M_{\odot}$. For the remaining calculations in this section (shown in Figs. 3 and 4) a switching mass of $0.7 M_{\odot}$ was used. We varied this value slightly for the purpose of testing, but it turned out to have little influence on the fitting of final system parameters.

We obtained four approximate solutions for the initial

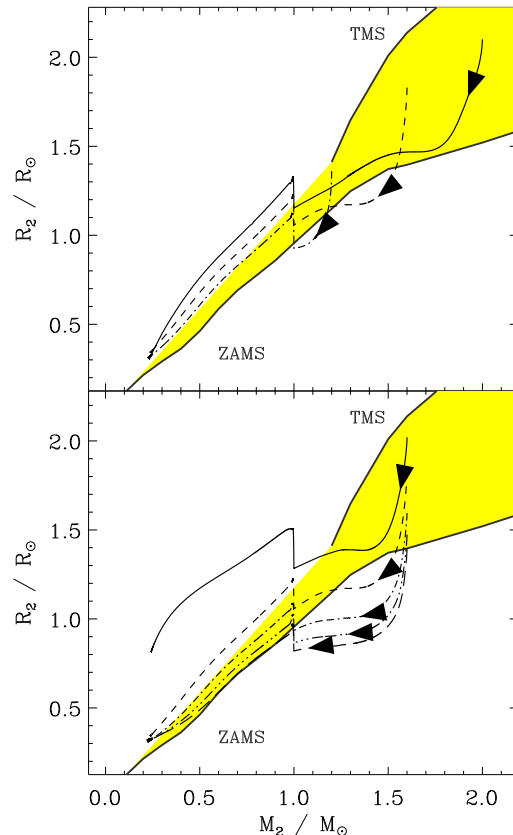


Figure 2. Single star calculations with a mass loss rate according to eq.(4). The upper panel shows the radius evolution of mass-losing stars with initially 1.2, 1.6, $2.0 M_{\odot}$ and an initial age 0.75 of their MS lifetime. The lower panel illustrates the variation with age for a $1.6 M_{\odot}$ star, covering an initial age of 0, 0.25, 0.5, 0.75 and 1 MS-timescale from bottom to top. Note that the strong deviation of the most evolved of the five tracks results from ongoing nuclear evolution, which is fast enough because the system was already close to entering the Hertzsprung gap. The grey shaded area and additional lines mark the location of the MS (as labelled). Thermal timescale mass transfer was switched off at $M_2 = 1.0 M_{\odot}$ in each of the computations.

parameters of AE Aqr (M_{2i}/M_{\odot} , X_{ci} , M_2/M_{\odot}): S1 (1.8, 0.18, 0.6), S2 (1.9, 0.21, 0.6), S3 (2.1, 0.23, 0.54) and S4 (2.3, 0.247, 0.5), which provided the starting point for the full binary calculations in the next section. A decreasing amount of initial core hydrogen fraction X_{ci} indicates a donor that is advanced further in its MS evolution. The tracks for S3 and S4 are shown in Figs. 3 and 4 as the evolution of spectral type over secondary mass and orbital period respectively.

The (admittedly crude) modelling presented in this section leads to an overall fitting end state of the system, i.e. a reasonable model for AE Aqr today. However the preceding transition phase is poorly modelled. As a general trend derived from comparing S1-S4, lower initial secondary masses require the donor to be a bit more evolved, and lead to a slightly higher current donor mass in AE Aqr. We can there-

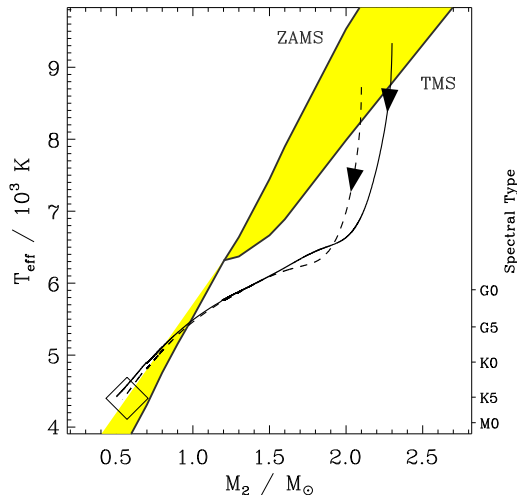


Figure 3. Evolution of effective temperature (spectral type) with decreasing mass in the two best-fitting single star models S3 with $M_{2i} = 2.1 M_{\odot}$ (dashed line) and S4 with $2.3 M_{\odot}$ (full line). Details of the conversion from T_{eff} to SpT are discussed in the text. Thermal timescale mass transfer was switched off at $M_2 = 0.7 M_{\odot}$ in accord with the actual WD mass in AE Aqr. Tracks end close to the current position of AE Aqr, marked by a diamond. Note that the direction of evolution of single stars on the MS (shaded area) is towards lower T_{eff} in more massive stars, but towards higher temperatures at lower masses.

Table 1. Summary of system parameters for selected full binary calculation.

| Name | M_{1i}/M_{\odot} | M_{2i}/M_{\odot} | X_{ci} | P_i/hr | η |
|------|--------------------|--------------------|----------|-----------------|--------|
| B1 | 0.95 | 2.35 | 0.287 | 17.9 | 0 |
| B2 | 0.95 | 2.1 | 0.223 | 18.5 | 0 |
| B3 | 0.95 | 1.8 | 0.190 | 18.1 | 0 |
| B4 | 0.8 | 2.35 | 0.287 | 17.5 | 0.1 |
| B5 | 0.6 | 1.6 | 0.560 | 10.8 | 0.3 |
| B6 | 0.6 | 1.6 | 0.087 | 18.6 | 0.3 |

fore expect initial values around $M_2 \sim 2 M_{\odot}$ to provide progenitors for AE Aqr.

4 FULL BINARY CALCULATIONS

There are two major effects suppressed by the single star treatment in the previous section:

(i) For identical initial donor stars, different initial WD masses and thus initial mass ratios can produce very different mass transfer rate histories, which are represented too simplistically by eq.(4).

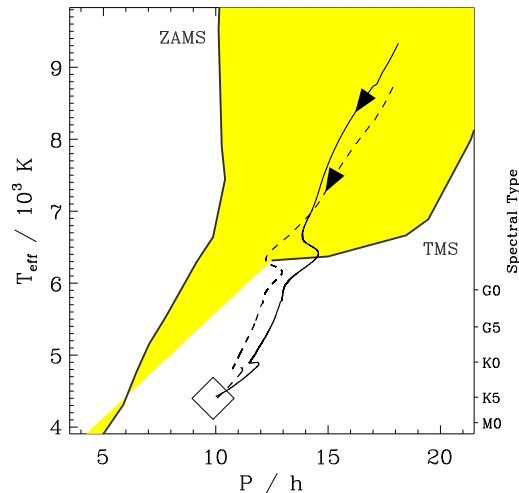


Figure 4. Evolution of effective temperature (spectral type) with orbital period, for the same two tracks S3 & S4 as in the previous figure. The large wiggles in orbital period during the early stage (at a SpT slightly above G0) are caused by the inconsistency introduced by an imposed mass transfer rate eq.(4), and the smaller ones near SpT K0 are directly connected with the jump in \dot{M}_2 . The exact MS location (shaded area) in orbital period is of course a function of the primary mass, for which we have assumed the canonical value of $M_1 = 0.89 M_{\odot}$ in this figure.

(ii) The growth of the WD mass is ignored in converting radii to orbital periods.

Therefore we have computed a range of tracks in a more self-consistent way. The mass transfer rate is calculated according to the current orbital parameters (‘full binary evolution’). The code used for this work is still based on the Kolb & Ritter (1992) version of Mazzitelli’s stellar evolution. The main challenge in computing the evolutions through and beyond a phase of thermal-timescale mass transfer lies in a proper treatment of numerical and physical instabilities.

We present here the results for six tracks, whose parameters are given in Table 1. In all cases the mass accretion efficiency η defined in eq.(1) is kept constant throughout the evolution. Conservative mass transfer ($\eta = 1$) is not considered (see Sect. 2). Figure 5 illustrates the variety of post-thermal-timescale mass transfer transitions mentioned in the discussion of the single star results above. Track B3 shows just a small bump of enhanced mass transfer. Increasingly S-shaped period loops appear in B2, B6, and B1. Tracks B5 and B4 show the beginning of an apparent runaway caused by a delayed dynamical instability (DDI); here extreme mass ratios coincide with sufficiently deep transient outer convection zones. None of these cases, including the dip in the mass transfer rate at the end of the thermal-timescale mass transfer found in B1, is adequately described by eq.(4).

The dominant parameter governing the behaviour along the sequence B3–B2–B6–B1–B5–B4 is the initial mass ratio: larger values correspond to stronger thermal instability. In

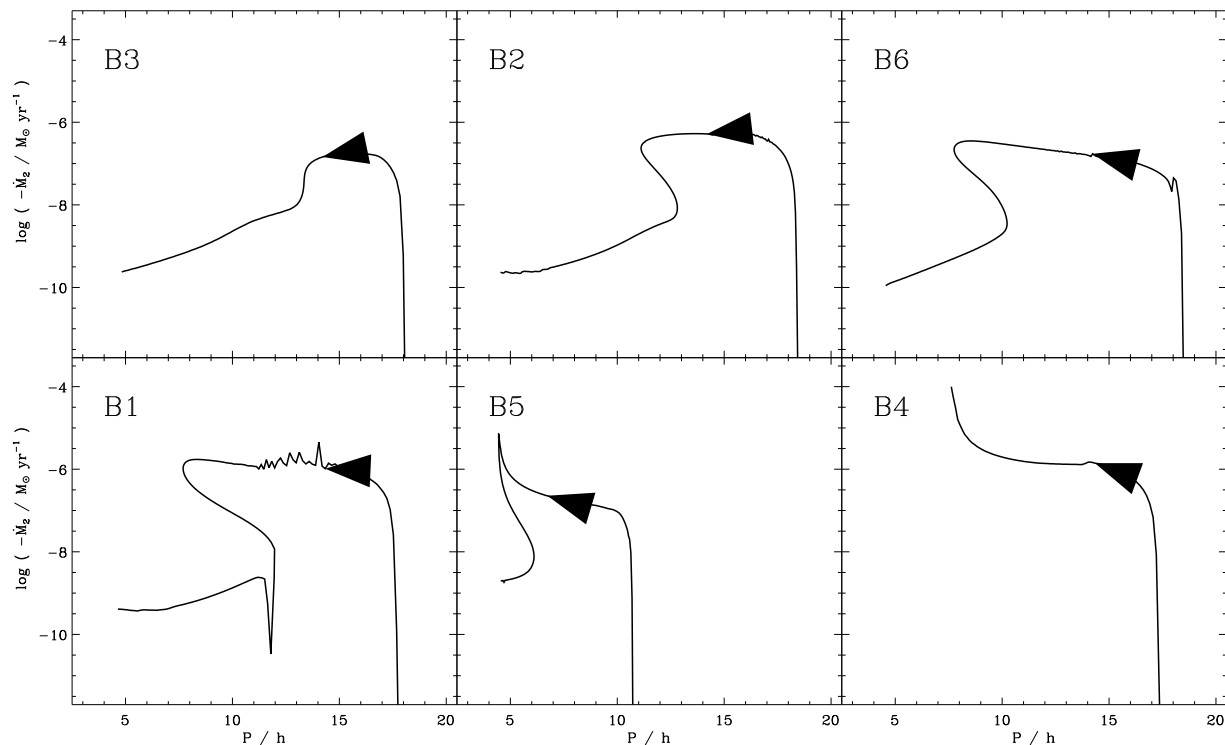


Figure 5. Possible transitions at the end of thermal-timescale mass transfer shown as the evolution of mass transfer rate over orbital period. Each panel is labelled according to system parameters given in Table 1. The features encountered include a simple drop in mass transfer rate (B3), a nose-like overhang (e.g. B6), up to cases suffering from an incipient delayed dynamical instability (DDI), countered just in time by the reversal of the mass ratio in one case (B5).

addition the choice of η (modifying the stability criterion) and the evolutionary state of the donor (e.g. B5–B6) can also have a strong impact on the evolutionary curves.

In some of the curves, particularly B1, a significant amount of numerical noise is apparent during the early high mass transfer rate phase. This is connected with the growth of an outer convective envelope caused by the rapid mass loss. As donors of these masses have initially radiative envelopes, very thin convective layers are present at the onset of this transition. This creates substantial numerical difficulties as minute discontinuities in the evolution of the star’s radius will be reflected in erratic jumps of the mass transfer rate. As time proceeds, the average thermal reaction of the star can be seen to pass right through the average of the scatter in \dot{M}_2 : various tests with enhanced resolution and reduced timesteps have confirmed that the subsequent structure of the star is unaffected from these problems, which are localized in layers close to the surface and thus have quite short thermal relaxation timescales.

Here we discuss tracks B1–B3 and B6. Figure 6 shows remarkable similarities to Fig. 3, except for the high initial mass ratio cases (B1 & B6) which evolve in a much wider arc back to the mass and SpT of AE Aqr. Inset (a) shows a zoomed part of the end region of the tracks (discussed in the next section), while inset (b) focusses on the region near the current position of AE Aqr (again marked

by an open diamond). Asterisks mark the position along each track where the observed mass ratio (presumably the best determined observable quantity besides orbital period) is matched. Given the uncertainties of spectral type calibration in the models and observational mass determinations, all four models qualify as potential progenitors. Not surprisingly the evolution vs orbital period shown in Fig. 7 has very different features from the corresponding Fig. 4: the loops and wiggles in the full binary plot correspond to the S-shaped curves shown in Fig. 5. Insets (a) and (b) again zoom in on regions of special interest, showing the rather good agreement with the observed values of AE Aqr. The jitter visible at the beginning of especially B2 results as discussed above from numerical difficulties at the onset of mass transfer from an outer convective envelope. Again the strong influence of a large initial mass ratio on the curves of B1 and B6 can be seen.

All tracks appear very non-MS like after passing through AE Aqr, which is a consequence of their advanced nuclear evolution. As listed in Table 1 and obvious from Fig. 7, the remaining core hydrogen content at the onset of mass transfer decreases with initial donor mass (B1–B2–B3–B6) in order to get near the current position of AE Aqr.

The full binary calculations in this section confirm the single star results for a range of suitable progenitors for AE Aqr. Evolutionary tracks for a variety of models do pass

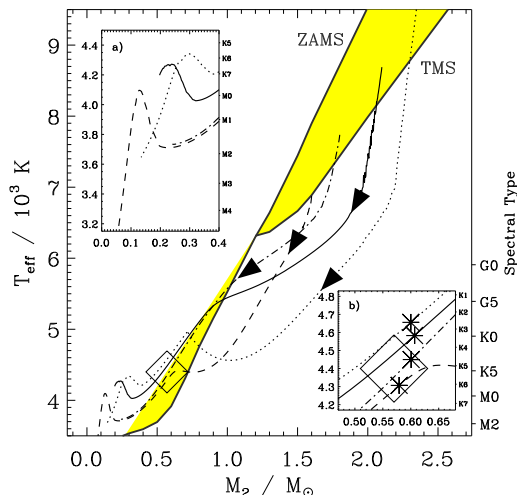


Figure 6. Tracks of models B1 (dotted), B2 (full), B3 (dash-dotted), and B6 (dashed) in the plane of effective temperature and secondary mass. The diamond marks the position of AE Aqr, the shaded area framed by thick lines indicates the MS. The insets provide a zoomed view of the end stages (a) and AE Aqr’s position today (b). In the latter, asterisks are used to mark the position along each track where the observed current mass ratio of AE Aqr is reached, showing a fair agreement between the system and the proposed progenitor models.

through the currently observed orbital period, spectral type, mass ratio and even individual masses M_1 and M_2 .

So far we have not used the additional constraints from other observational properties of AE Aqr. These distinguish between different scenarios.

5 PROPERTIES OF CVS DESCENDING FROM SUPERSOFT BINARIES

5.1 The WD spin

We first consider the current accretion state in AE Aqr. The rapidly rotating WD ($P_{\text{spin}} = 33$ s) is spinning down on a timescale of $\sim 10^7$ yr, consistent with powering the mass expulsion in the propeller phase (Wynn et al., 1997). As the timescale for the spin to reach equilibrium with the mass transfer rate is $\lesssim 10^7$ yr, the high mass transfer rate which spun up the WD must have ended only about 10^7 yr in the past. Figure 8 compares the mass transfer rate evolution for the four full binary models (B1–B3, B6). Clearly all cases predict the right \dot{M}_2 , but all except one (B6) take too much time to reach that position. The spindown properties therefore clearly favour a large initial mass ratio for the progenitor of AE Aqr, and some fractional mass accumulation (here an average of 0.3) on to the WD during the supersoft thermal–timescale mass transfer phase.

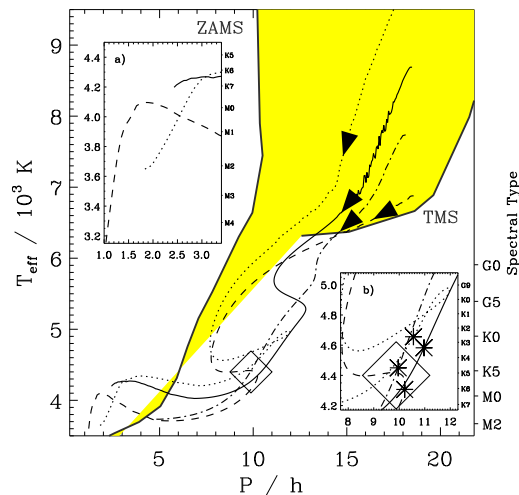


Figure 7. Tracks of models B1 (dotted), B2 (full), B3 (dash-dotted), and B6 (dashed) in the plane of effective temperature and orbital period. As in Fig. 4 above, the position of AE Aqr and the location of the MS are indicated. Similarly insets provide a zoomed view of the end stages (a) and the AE Aqr position today (b), in which once again asterisks (marking the observed current mass ratio of AE Aqr) confirm the successful modelling.

5.2 Abundances

Another potential way to distinguish between the models lies in their different initial masses and central hydrogen fractions. If we combine the observations of the extreme UV line ratios of CIV and NV with the apparent oversize of the donor for its spectral type (long orbital period), the natural explanation is chemical evolution of the stellar interior. Given the complex convective history and the different initial core masses and compositions of our four cases, we can construct e.g. an evolutionary sequence of characteristic surface elements as shown in Fig. 9. Despite the loss of more than a solar mass from the donor, solar composition is still maintained for a long time in sequence B2. Later however the ratios of ^{12}C to ^{13}C and C to N decrease by more than one or two orders of magnitude respectively. Vertical lines mark the point in the evolution where the orbital period and mass ratio of AE Aqr are matched: clearly this sequence provides more than enough C depletion to explain the UV observations of Jameson et al. (1980). Very similar results are found in the other cases. Bearing in mind that B2 was not a particularly strong case of thermal–timescale mass transfer, it seems very likely that chemical anomalies like these are quite common in post–thermal–timescale mass transfer systems.

In order to understand the origin of this specific form of change in the C/N ratio, we take a closer look at the internal structure of sequence B3 in Fig. 10. Mass transfer in this sequence started with a $1.8M_{\odot}$ donor having only 19% hydrogen left in the core. The left panel of Fig. 10 shows the internal profile of C/N shortly after filling the Roche

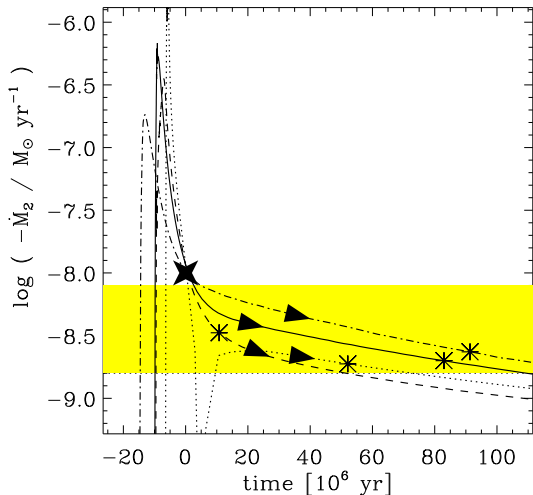


Figure 8. Time evolution of the mass transfer rate of the model sequences B1 (dotted), B2 (full), B3 (dash-dotted), and B6 (dashed) shown in the previous figures. After a brief ($\lesssim 10^7$ yr) phase of high mass transfer rates, the system settles towards its current rate. Each track reaches the current mass ratio $q = 0.64$ at the position marked by an asterisk within the shaded region which covers the estimated range of the current mass transfer rate. The time axis is offset such that all tracks pass through the beginning of the spindown phase (marked by the spiked cross and assumed to start at $10^{-8} M_{\odot} \text{ yr}^{-1}$) at time $t = 0$. Larger values of the initial mass ratio q_i accelerate the decline and thus shorten the delay between spin-up and the currently observed propeller state, leaving model B6 as the most suitable progenitor system.

lobe, with mass $M_2 = 1.69 M_{\odot}$. The initial solar composition has been modified severely by nuclear burning and subsequent mixing in the central $\lesssim 1 M_{\odot}$. Although substantial energy generation by CNO burning is limited to the very central regions (especially the convective core plateau in the inner $\sim 0.1 M_{\odot}$), the relatively long duration of the previous MS lifetime has allowed the nuclear reactions to change the composition much further out. The temperature-dependent CNO equilibrium ratios have been reached out to $0.6 M_{\odot}$, whereas the slower nuclear reactions beyond that have only started to reduce the amount of C. Once thermal-timescale mass transfer sets in however, this chemical profile remains frozen (everything happens within $\leq 10^7$ yr, cf. Fig. 8). Material is removed layer by layer from the top, until finally an outer convection zone starts to penetrate the chemically modified region, or the region itself is laid bare already. The right panel of Fig. 10 illustrates this, when only $M_2 = 0.69 M_{\odot}$ is left. The C/N ratio in the small surface convection zone is more than a factor of 100 below solar, i.e. even the weakest thermal-timescale mass transfer in case B3 has no trouble explaining the anomalous composition of AE Aqr.

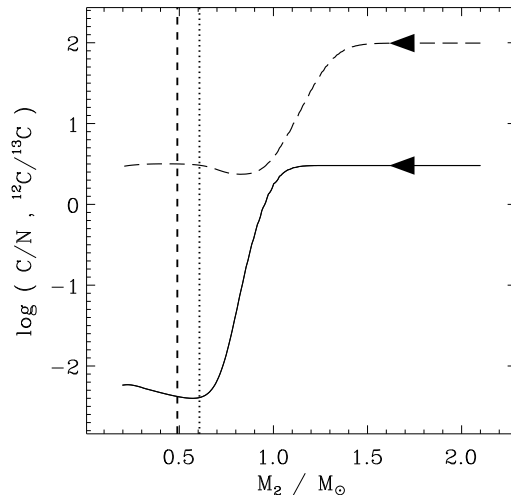


Figure 9. Change of surface chemical composition in sequence B2: The system evolves from right to left. After an initial phase of constant (solar) composition, the ratios of both C/N (lower curve) and C-12/C-13 (upper curve, dashed) drop severely as the outer convective envelope reaches down into previously CNO-burning regions. Vertical lines mark the position where the sequence reaches the orbital period (dashed) and mass ratio (dotted) of AE Aqr respectively.

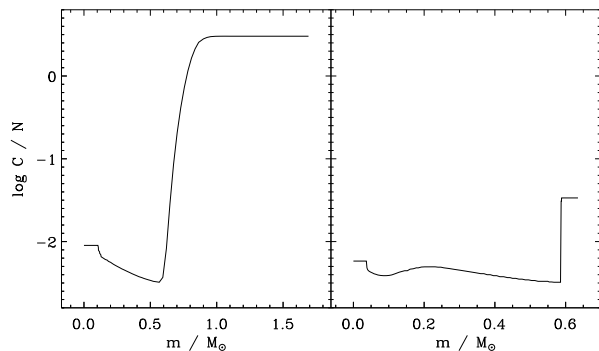


Figure 10. Internal C/N ratio profile taken from two models of sequence B3. The lefthand panel shows the situation at $M_2 = 1.69 M_{\odot}$ during thermal-timescale mass transfer, while the model in the righthand panel at $M_2 = 0.69 M_{\odot}$ is a close representation of AE Aqr now. Note the reduction of the surface ratio by a factor of ~ 120 once mass loss has removed the solar composition layers completely.

5.3 Evolutionary endpoints: the AM CVn systems

The later stages and endpoints of the evolutionary scenarios found for AE Aqr are connected to the advanced initial stage of nuclear burning on the MS. As the insets (a) in Figs. 6 and 7 show, the most extreme case B6 (and quite similar B3, which has been stopped around $P_{\text{orb}} = 5$ hr) reach an orbital period of 60 min or below. In this state the

donors consist largely of helium produced during detached MS burning. Thus these systems qualify as AM CVn systems or at least intermediate cases such as V485 Cen (Augusteijn et al., 1996). An almost identical channel of forming ultra-compact binaries has recently been studied by Podsiadlowski et al. (2001), focussing on initial donor masses below $1.4 M_{\odot}$ and binary population synthesis aspects.

5.4 Other properties

(i) The upper limit for the donor mass that potentially leads to similar evolutionary tracks is determined by the occurrence of a DDI, and the requirement of a strong braking mechanism at the end of the thermal-timescale mass transfer supersoft phase. Both are extremely sensitive to the amount of mass accreted during the high \dot{M}_2 episode, which certainly needs further investigation. We suggest that masses up to $2 M_{\odot}$ should be considered.

(ii) After passing the state exemplified by AE Aqr, all donor stars in our models have spectral types too late for their orbital periods. Hence post-thermal-timescale mass transfer systems provide a natural explanation for the apparently evolved state of many CVs with periods above 6 hr (Baraffe & Kolb, 2000). Podsiadlowski et al. (2001) claim agreement between the properties of their population and the observed SpT distribution in CVs (Beuermann et al., 1998).

(iii) A simple argument (King & Schenker, 2002) implies a substantial number of evolved systems among CVs: at the borderline between systems brought into contact by some form of braking and those by nuclear evolution there will always be donors which have almost finished their MS phase, but are still kept at short orbital periods by a thermal-timescale mass transfer phase followed by normal angular momentum loss driven evolution.

(iv) Most importantly, AE Aqr seems to be living proof that this kind of evolution does exist. If (as we strongly suspect; see below) a large number of systems with similar properties have passed through such a phase, the same group of systems may account for short-period supersoft binaries, AM CVns, V485 Cen-type close binaries, and a substantial fraction of CVs. Although these probably include unusual ones like AE Aqr or V1309 Ori, many of them may appear fairly normal.

(v) If we assume the track of B6 as shown in Fig. 8 as typical for all supersoft, AM CVn, and AE Aqr-like stages, one would expect roughly equal durations of the supersoft and spindown phases. The subsequent lifetime as normal CV above the period gap is about 100 times longer. More difficult to estimate is the fraction of post-TTMT systems that end up as AM CVn stars: the uncertainties of post-common envelope distributions, DDI, and magnetic braking issues prevent serious quantitative predictions. Direct comparison with observed statistics is further complicated by poorly understood selection effects in these different classes.

A related question concerns the expected fraction of post-thermal-timescale mass transfer systems among CVs. We make a simple estimate using recently improved fits to the Galactic mass function (Chabrier, 2001), which enter as the distribution of initial donor star masses between $0.1 M_{\odot}$ and $2.1 M_{\odot}$. The upper limit is set by the onset of delayed dynamical instability ($q_i = 3$) for a white dwarf mass fixed for

simplicity at $0.7 M_{\odot}$. Assuming that these systems evolve as normal CVs for $q_i < 1$ and via thermal-timescale mass transfer for $q_i > 1$ we find that in a steady state about one-third of current CVs should be post-thermal-timescale mass transfer systems. As a simple correction for the reduced binary fraction at low masses we have applied a weighting factors of 0.7 (for the thermal-timescale mass transfer mass range) and 0.3 (for normal CV donor masses). While this is obviously a fairly crude estimate, it does strongly suggest that a substantial fraction of CVs could show signs of an earlier thermal-timescale mass transfer phase. We note that more exhaustive studies of CV formation lead to roughly similar results. For example Table 1 from de Kool (1992) indicates that a large fraction (if not a majority) of zero-age binaries will undergo thermally unstable mass transfer rather than becoming a CV directly.

6 CONCLUSION

We have shown that the assumption of thermal-timescale mass transfer in the recent past of AE Aqr provides plausible explanations for all of its current observational properties. The system parameters for the best-fitting progenitor model presented in this paper (B6) are $M_{2i} = 1.6 M_{\odot}$ (fairly far evolved on the MS) and $P_i = 18.6$ hr with a primary of $M_{1i} = 0.6 M_{\odot}$ which manages to accrete about 30% of the total transferred mass upon reaching the current phase of AE Aqr. This indicates a relatively large initial mass ratio, and some fraction of mass accretion during the thermal-timescale mass transfer phase. Although the precise values may change, the idea is very robust, as the differential results from Sect. 3 & 4 clearly indicate that it will be always possibly to end up with an excellent model for AE Aqr.

The short duration of the thermal-timescale mass transfer and the transition stage (where AE Aqr currently is) implies a large birthrate, and thus suggests a large number of systems passing through similar evolutions. We expect descendants from systems similar to AE Aqr, and thus from supersoft binaries, to form a substantial fraction of the currently known CVs. The contortions of the $-\dot{M}_2 - P$ curves of Fig. 5 suggest that non-magnetic descendant systems may change between recurrent novae, novalike and dwarf nova behaviour during and after the transition from thermal-timescale mass transfer to normal CV evolution. Descendants with significant WD magnetic fields will also appear in various guises during these phases. We suggest that the long-period AM Her system V1309 Ori (Schmidt & Stockman, 2001; Staude et al., 2001) is a descendant of a supersoft binary, cf. King et al. (2002). This system is apparently able to synchronise at its unusually long period of 8 hr because of the drop in mass transfer rate at the end of the thermal-timescale mass transfer phase. The pulsing supersoft source XMMU J004319.4+411758 found by XMM in M31 may be an example of a progenitor still in the thermal-timescale mass transfer phase (King et al., 2002). Note that V1309 Ori, the slightly nonsynchronous polar BY Cam (Bonnet-Bidaud & Mouchet, 1987) and the intermediate polar TX Col (Mouchet et al., 1990) all show high Nv/CIV ratios similar to AE Aqr. Abundance anomalies possibly related to stripping of a partially evolved com-

panion were suggested by Mouchet et al. (1990) in the latter two cases.

We conclude that in spite of its apparent uniqueness, AE Aqr is only the first confirmed member of a much larger population of post-supersoft binaries, constituting a significant fraction of all CVs. A way of checking for this population is to determine the C/N ratio by measuring CIV 1550 versus NV 1238. A low value here will be strongly suggestive of descent from a supersoft binary.

ACKNOWLEDGEMENTS

Theoretical astrophysics research at Leicester is supported by a PPARC rolling grant. ZZ was supported by Royal Society China Joint Project Q760.

References

- Augusteijn, T., van der Hooft, F., de Jong, J. A., & van Paradijs, J.: 1996, *A&A* 311, 889
- Baraffe, I. & Kolb, U.: 2000, *MNRAS* 318, 354
- Beuermann, K., Baraffe, I., Kolb, U., & Weichhold, M.: 1998, *A&A* 339, 518
- Bonnet-Bidaud, & J.M., Mouchet, M., 1987: *A&A*, 188, 89
- Casares, J., Mouchet, M., Martínez-Pais, I. G., & Harlaftis, E. T.: 1996, *MNRAS* 282, 182
- Chabrier, G.: 2001, *ApJ* 554, 1274
- de Jager, O. C., Meintjes, P. J., O'Donoghue, D., & Robinson, E. L.: 1994, *MNRAS* 267, 577
- de Kool, M.: 1992, *A&A* 261, 188
- Jameson, R. F., King, A. R., & Sherrington, M. R.: 1980, *MNRAS* 191, 559
- King, A. R.: 1988, *QJRAS* 29, 1
- King, A. R., Osborne, J. P., & Schenker, K.: 2002, *MNRAS* 329, L43
- King, A. R. & Ritter, H.: 1999, *MNRAS* 309, 253
- King, A. R. & Schenker, K.: 2002, in B. T. Gänsicke, K. Beuermann, & K. Reinsch (eds.), *The Physics of Cataclysmic Variables and Related Objects*, ASP Conference Series Vol. 261, San Francisco, 233–241
- King, A. R., Schenker, K., Kolb, U., & Davies, M. B.: 2001, *MNRAS* 321, 327
- Kolb, U. & Ritter, H.: 1992, *A&A* 254, 213
- Mauche, C. W., Lee, Y. P., & Kallman, T. R.: 1997, *ApJ* 477, 832
- Mazzitelli, I.: 1989, *ApJ* 340, 249
- Mouchet, M., Bonnet-Bidaud, J.M., Hameury, J.M., & Acker, A.: 1990, in *Evolution in Astrophysics: IUE Astronomy in the Era of New Space Missions*, ESA, 423–426
- Podsiadlowski, P., Han, Z., & Rappaport, S.: 2001, *MNRAS* submitted (astro-ph/0109171)
- Pylyser, E. & Savonije, G. J.: 1988a, *A&A* 191, 57
- Pylyser, E. H. P. & Savonije, G. J.: 1988b, *A&A* 208, 52
- Schenker, K.: 2001, in P. Podsiadlowski, S. Rappaport, A. R. King, F. D'Antona, & L. Burderi (eds.), *Evolution of Binary and Multiple Star Systems*, ASP Conference Series Vol. 229, San Francisco, 321–332
- Schenker, K. & King, A. R.: 2002, in B. T. Gänsicke, K. Beuermann, & K. Reinsch (eds.), *The Physics of Cataclysmic Variables and Related Objects*, ASP Conference Series Vol. 261, San Francisco, 242–251
- Schmidt, G. D. & Stockman, H. S.: 2001, *ApJ* 548, 410
- Sobermann, G. E., Phinney, E. S., & van den Heuvel, E. P. J.: 1997, *A&A* 327, 620
- Staude, A., Schwope, A. D., & Schwarz, R.: 2001, *A&A* 374, 588
- van den Heuvel, E. P. J., Bhattacharya, D., Nomoto, K., & Rappaport, S. A.: 1992, *A&A* 262, 97
- Webbink, R. F.: 1985, in J. E. Pringle & R. A. Wade (eds.), *Interacting Binary Stars*, Chapt. 2.2, 39–70, Cambridge Univ. Press, Cambridge
- Welsh, W. F.: 1999, in *Annapolis Workshop on Magnetic CVs*, ASP Conference Series Vol. 157, San Francisco, 357–367
- Welsh, W. F., Horne, K., & Gomer, R.: 1993, *ApJ* 410, L39
- Welsh, W. F., Horne, K., & Gomer, R.: 1995, *MNRAS* 275, 649
- Wynn, G. A., King, A. R., & Horne, K.: 1997, *MNRAS* 286, 436